Appl. Sci. Converg. Technol. 24(6): 228-231 (2015)
http://dx.doi.org/10.5757/ASCT.2015.24.6.228

Research Paper

Initial growth mode of ultra-thin Al films on a W(110) surface at high temperatures

Dae Sun Choi* and Mi Mi Park*
**Department of Physics, Kangwon National University, Chunchon Kangwon do 200-701 South Korea*

Received November 9, 2015; revised November 20, 2015; accepted November 20, 2015

Abstract We investigated the adsorption structures and the initial growth mode of ultra-thin Al films on a W(110) surface at a high temperature. When Al atoms were adsorbed on the W(110) at the substrate temperature of 1100 K and with coverage of 0.5 ML, Al atoms formed a p(2×1) double-domain structure. When the coverage was 1.0 ML, the double domain of a hexagonal structure (fcc(111) face) rotated ±5° from the [100] direction of the W(110) surface and another distorted hexagonal structure were found. Low-energy electron diffraction results along with ion scattering spectroscopy results showed that the Al atoms followed the Volmer-Weber growth mode at a high temperature.

Keywords: Al, W(110), Adsorption Structure, Growth mode

I. Introduction

Owing to the dangling bonds on a substrate surface, the interactions between adsorbates and the substrate surface differ somewhat from interactions among bulk atoms. Therefore, ultra-thin films on a single-crystal substrate show various geometrical characteristics. Many thin-film structures with crystal structures that differ from the substrate structures have been studied [1-3]. In particular, face-centered cubic (fcc) materials on body-centered cubic (bcc) materials have long been a subject of interest due to their different crystal structures and the resulting lattice mismatch [4-10].

For the development of nano-scale devices, it is important to investigate the initial growth mode. Therefore, the investigation of the initial growth mode of fcc adsorbates on bcc substrates is a worthwhile endeavor. Although interesting studies of Al adsorption on W single crystals have been reported in the literature [11,12,13], and a study of the Al/W(100) surface at 850 C also exists [14], the growth mode of the Al/W(110) system at temperatures higher than 1000 K has not yet been reported.

It is known that bcc W has a high melting point and that it can be easily cleaned and reused for repeated experiments. Aluminum has an fcc structure and a low melting point and therefore can be readily evaporated using a filament-type evaporator. Therefore, Al/W is a good system with which to investigate the growth mode of fcc materials on bcc materials. A single-crystal surface has many different adsorption sites. Although these adsorption sites are geometrically identical, the electron orbital configurations on the sites are not the same. Tungsten has $5d^4\ 6s^2$ electrons, and the s and d bands overlap. Thus, tungsten single-crystal surfaces have various electron orbital configurations according to the crystal faces. With regard to the W(100) surface, there are four different electron orbital configurations, and combinations of these orbital configurations result in various set of identical adsorption sites [15]. A detailed electron configuration model is discussed in the results and discussion section.

In this study, we investigated the growth mode of aluminum atoms adsorbed on a W(110) surface at a temperature of 1100 K. We found that Al atoms form a p(2×1) structure when the coverage is 0.5 ML; when the coverage is 1.0 ML, three different structures were revealed, and Al grew in the Volmer-Weber mode [16].

Corresponding author; dschoi@kangwon.ac.kr

II. Experiment

Our experimental system included ion scattering spectroscopy (ISS), and low-energy electron diffraction (LEED), and was equipped with a residual gas analyzer (RGA), a filament-type Al evaporator with a shutter, and an electron beam heating sample holder. For materials with high melting points, an electron beam heating evaporator is useful, but for Al with a low melting point, a filament-type evaporator is convenient because it does not require a high-voltage power supply.

The base pressure of our experimental system was 5×10^{-11} torr and the pressure during the Al evaporation step was ~5×10^{-9} torr. The diameter of the W(110) substrate was 1

*Corresponding author
E-mail: dschoi@kangwon.ac.kr

cm and its thickness was 3 mm. The W substrate was cleaned according to previously published cleaning methods [17,18,19,20]. It is known that an oxygen treatment is useful for removing any contaminated carbon [17]. In any cases of carbon contamination, we carried out oxygen treatments using the flash method. The coverages were estimated from the He^+ back-scattering intensity of the Al and W atoms obtained via ISS. In these estimations, we considered the scattering cross-sections [21]. Al atoms were adsorbed onto the W(110) surface at the substrate temperature of 1100 K. The deposition rate was controlled by adjusting the filament current, and the thickness was controlled using a mechanical shutter. The Al deposition rate was 0.1 ML/min. The samples were heated using the electron beam heating method, and the sample temperatures were measured with an optical pyrometer.

III. Results and Discussion

Figure 1 shows the LEED patterns of (a) clean W(110), (b) 0.5 ML Al/W(110), (c) 1.0 ML Al/W(110), and (d) 1.5 ML Al/W(110) surfaces when the substrate temperature was maintained at 1100 K during the Al deposition step.

1. 0.5 ML Al/W(110)

The LEED pattern of the 0.5 ML Al/W(110) sample surface showed a p(2×1) double-domain structure. To explain the p(2×1) structure, schematic representations of (a) a clean W(110) LEED image, and (b) a 0.5 ML/W(110) surface image are shown in Figure 2. Figure 2(c) illustrates how this p(2x1) double-domain image was formed.

Although the adsorption sites appear to be identical geometrically, if we consider the electron orbital configuration, the potential energy of these sites differs.

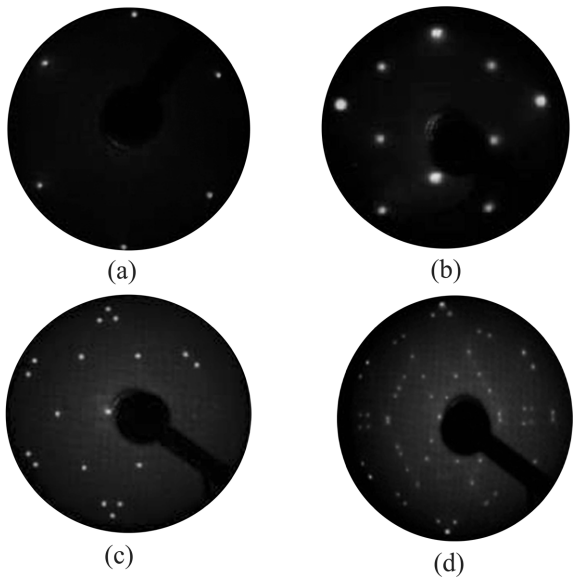

Figure 1. LEED patterns of (a) clean W(110), (b) 0.5 ML Al/W(110), (c) 1.0 ML Al/W(110), and (d) 1.5 ML Al/W(110) surfaces.

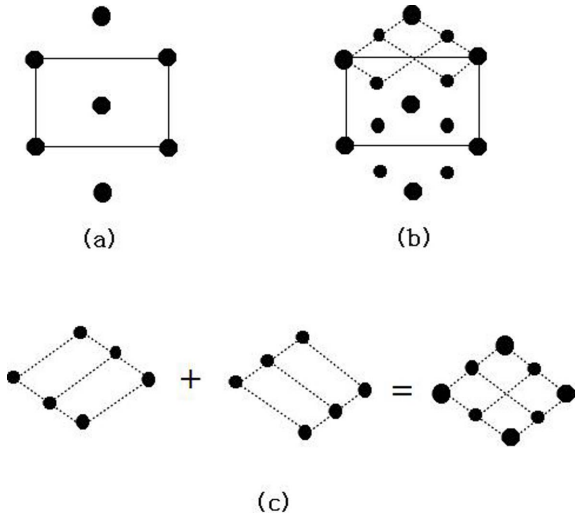

Figure 2. Schematic LEED patterns of (a) a clean W(110) surface and (b) a p(2×1) double-domain LEED pattern; the dashed circles show the p(2×1) double domain and (c) shows the formation of a p(2×1) pattern.

Tamm et al. [22] reported that tungsten 5d and 4s bands overlap in terms of their energy; therefore, new types of orbitals are formed by the hybridization of the d and s orbitals. Their orbital model successfully explains various adsorption structures [16].

For the W(100) surface, there are four non-bonding d orbitals on the surfaces; if these d orbitals hybridize with s orbitals, there are many different adsorption sites, resulting in many different adsorption structures, such as p(2×2), c(2×2), and c(4×4). For the W(110) surface, the interaction between adsorbates and the W substrate is simpler because there two non-bonding d orbitals on the surface. This may explain why the adsorption structure of a W(100) surface is more multifarious than that of a W(110) surface. Figures 3(a) and (b) show the bonding orbitals of the W(110) surface drawn considering Tamm's report. There are two different sites; that is, the sites labeled A and B are not identical and either the A or the B site forms p(2×1) structures (see the arrows in the figure). Koetter et al. [12] reported that for Al atoms adsorbed on long bridge sites, the adsorption height was 2.38 Å, and the lowest potential energy at the equilibrium position of the Al atom on the W(110) surface was −5.2 eV. On the Al(111) surface, it was −3.1 eV. This indicates that, in Koetter's work, adsorbed Al atoms form three-dimensional islands but do not cover the W(110) surface uniformly. Although their calculations were carried out for a single Al atom, they are still feasible for use in our system because the coverage in our system is very low.

Finally, we concluded that when Al atoms were adsorbed on the W(110) surface when the substrate temperature was maintained at 1100 K, Al atoms formed a p(2×1) structure and Al atoms adsorbed on the long bridge site. The adsorption model of the 0.5 ML Al/W(110) surface at a substrate temperature of 1100 K is shown in

Figure 3(c). If this structure is represented in a matrix form, the structure is $\begin{pmatrix} 2 & 0 \\ 0 & 1 \end{pmatrix}$ in a real lattice space. Our adsorption model is in good agreement with Kotter's theoretical results.

2. 1.0 ML Al/W(110)

The LEED pattern shown in Figure 1(c) differs somewhat from that of the 0.5 ML Al/W(110) sample. These patterns show four different structures: two domains of fcc(111) faces, a bcc(110) face, and an image of a distorted hexagonal structure.

Simple calculations show that the structure of the distorted hexagonal image has the $\begin{pmatrix} 2 & -1 \\ -1 & 2 \end{pmatrix}$ structure in a real lattice space. If the adsorbed Al atom covered the W(110) surface uniformly, the LEED image of the 1.0 ML Al/W(110) surface should not appear as a clean W(110) surface. However, this image still shows the bcc(110) surface. Figure 4(a) shows a schematic of the LEED image shown in Figure 1(c). To simplify, the distorted hexagonal image that appears in the center of the LEED image is shown separately in (b). As shown in Figure 4(a), the spots induced by Al atom adsorption show fcc(111) faces. If the adsorbed Al atoms form only one layer on the W(110) surface, these atoms will form a face close to the bcc (110) face rather than the fcc(111) face because Al atom-W(110) surface interaction is much stronger than that of the Al atom-Al(111) surface. If the Al atoms form three-dimensional islands, the interaction between the W(110) surface and the Al atoms on the highest layer of the islands will be weak. Therefore, the interaction between the Al atoms on the highest layer and the Al atoms on the next layer is stronger than that of the Al atoms on the highest layer and the W(110) surface. This result indicates that Al atoms do not cover uniformly but form three-dimensional Al islands. Therefore, the LEED results show the image of the clean W(110) surface overlapping with the image of the two-domain Al(111) surface and the distorted hexagonal structure. The $[1\bar{1}0]$ azimuth direction of the grown Al (111) surface was rotated ±5° from the [001] direction of the W(110) substrate surface. The bonding orbital model cannot explain the $\begin{pmatrix} 2 & -1 \\ -1 & 2 \end{pmatrix}$ structure and the double-domain hexagonal LEED image. If we remember that the p(2×1) phase appeared at coverage of 0.5 ML and disappeared at coverage of 1.0 ML, the $\begin{pmatrix} 2 & -1 \\ -1 & 2 \end{pmatrix}$ structure should be induced on the p(2×1) base structure. However, the p(2×1) base structure still cannot explain the $\begin{pmatrix} 2 & -1 \\ -1 & 2 \end{pmatrix}$ structure and the fcc(111) face Al island. Therefore, we suggest that buffer layers between the p(2×1) layer and the islands showing the hexagonal face layer and the distorted hexagonal image should be induced by three-dimensional Al islands. This assumption of buffer layers can be applied to the fcc(111) face Al islands. Because the W(110) image still appears in Figs. 1(c) and (d), the suggested buffer layers exist on the Al island but not on the entire substrate surface. This suggests that there are three growth modes: the Volmer-Weber (VW) mode, in which the adsorbed atoms form three-dimensional islands; the Stranski-Krastanov (SK) mode, in which the adsorbed atoms form three-dimensional islands after forming two-dimensional layers; and the Frank-Van der Merwe (FM) mode, in which adsorbed atoms grow layer by layer [16]. The results of our experiments strongly suggest that Al grew in the VW mode. It is interesting to note that the Al grew according to the FM mode when the substrate was at room temperature [13], whereas it was in the VW mode when the substrate temperature was high.

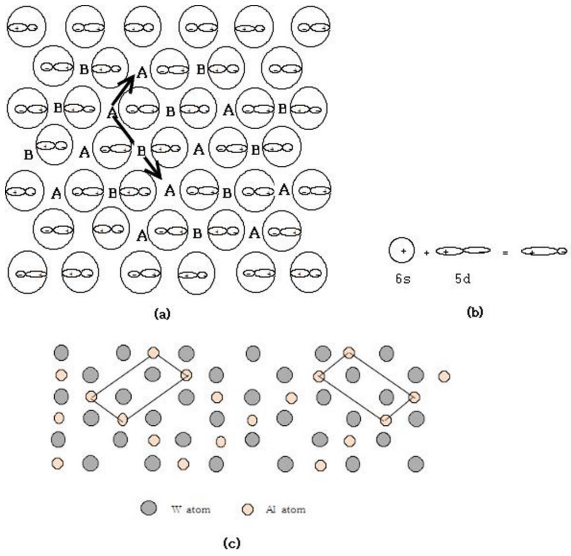

Figure 3. (a) Bonding orbitals of a W(110) surface drawn considering Tamm's report. Although sites A and B are geometrically identical, the bonding orbital model shows they are not actually identical sites. The arrows indicating A form a p(2×1) structure. (b) Schematic diagram of the orbitals formed by the hybridization of a 5d orbital with a 6s orbital. (c) The adsorption model of the p(2×1) double-domain Al/W(100) surface.

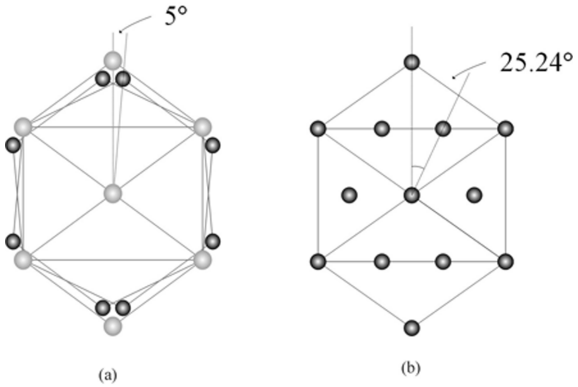

Figure 4. (a) Schematic drawing of the double-domain fcc(111) structure appearing in Figure 1(c). (b) Schematic drawing of the distorted hexagonal LEED spots appearing at the center of Figure 1(c). The distorted hexagonal pattern has a $\begin{pmatrix} 2 & -1 \\ -1 & 2 \end{pmatrix}$ structure in a real lattice space.

3. 1.5 ML Al/W(110)

As shown in Figure 1(c), many spots appeared in this system. Among these spots, we could find those induced by the structures appearing on the 1.0 ML Al/W(110)

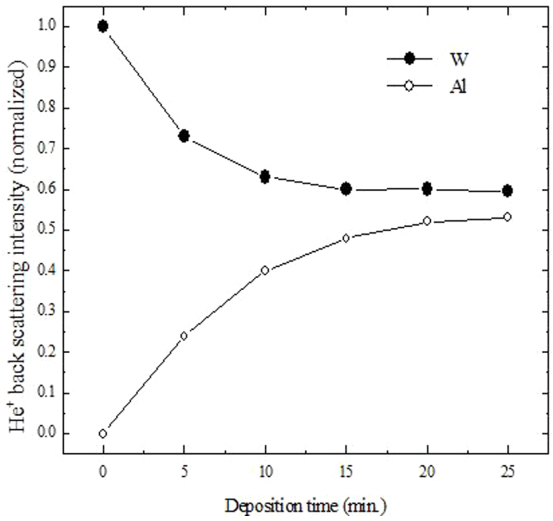

Figure 5. Back-scattering intensity of the He^+ from the Al/W(110) surface according to the deposition time. The intensities were normalized to the W signal when the Al coverage was 0.0 ML.

surface, that is, the bcc(110) surface, $\begin{pmatrix} 2 & -1 \\ -1 & 2 \end{pmatrix}$ structure and the two-domain Al(111) surface. In addition to these spots, we observed many adjacent new spots, indicating a long-range ordered structure in a real lattice space. Although analyzing these spots was overly complicated, it is clear that a clean W(110) surface appeared, indicating that Al grew in the VW mode. It is interesting that the p(2×1) structure appearing at the coverage of 0.5 ML disappeared when the coverage increased to 1.0 ML, whereas the fcc(111) structure and the $\begin{pmatrix} 2 & -1 \\ -1 & 2 \end{pmatrix}$ structure appearing at the coverage of 1.0 ML did not disappear when the coverage increased to 1.5 ML. However, the 1.5 ML Al/W(110) surface contained many long-range complex structures as well as structures appearing at the coverage of 1.0 ML. We expected that new Al atoms were adsorbed on the sites between the Al atoms forming the $\begin{pmatrix} 2 & -1 \\ -1 & 2 \end{pmatrix}$ structure and that this structure would become a more simple (a short-range ordered) structure, such as $\begin{pmatrix} 1 & -1 \\ -1 & 1 \end{pmatrix}$. However, these types of short-range ordered structures did not appear, indicating that these two phases were relatively stable.

Figure 5 shows the back-scattering intensity of the He^+ from the Al/W(110) surfaces according to the deposition time. The data points are normalized to the W peak obtained when the Al coverage is 0.0 ML, that is, a clean W(110) surface. As was expected, the W intensity decreased with an increase in the Al deposition time. One of the characteristics of low-energy ISS is surface sensitivity. The low-energy ion cannot penetrate the third layer or penetrate lower than the surface. For the W(110) surface, ions can penetrate into the second layer at the normal incident angle. Although penetration into the third layer is possible, the back-scattering probability from the third layer is extremely low. If we recall the deposition rate of 0.1 ML/min, the Al coverage at the deposition time of 25 minutes is 2.5 ML. If Al atoms cover the W(110) surface uniformly with multiple layers (2.5 ML), low-energy ions cannot penetrate into the W layers below the adsorbed Al layers and the ions scattered from the W layers below the Al layers are not likely to be detected. However, the W peak was still strong at the 2.5 ML Al/W(110) surface, indicating that the adsorbed Al atoms did not cover the W(110) surface uniformly but formed three-dimensional islands, revealing the clean W(110) surface. Therefore, we conclude that Al grows via the VW mode.

Conclusions

We investigated the growth mode of ultra-thin Al films on a W(110) surface. When the Al coverage was 0.5 ML and the substrate temperature was maintained at 1100 K, the adsorbed Al atoms covered the W surface uniformly and formed a p(2×1) double-domain structure. When the coverage was 1.0 ML, the adsorbed Al atoms formed three-dimensional islands and the Al adsorbed W(110) surface revealed a partially clean W(110) surface, which means that the Al grew in the VW mode. The 1.0 ML Al/W(110) surface had two different structures. One structure consisted of Al islands of the two-domain fcc(111) face. The $[1\bar{1}0]$ azimuth direction of the grown Al(111) surface was rotated ±5° from the [001] direction of the W(110) substrate surface. The second structure was the $\begin{pmatrix} 2 & -1 \\ -1 & 2 \end{pmatrix}$ structure. When the coverage was 1.5 ML, many complicated structures formed, and three structures appeared at the coverage of 1.0 ML. The ISS experiment also showed that the Al atoms on the W(110) surface grew according to the VW mode at 1100 K.

Our results will be useful in studies of the early growth stages of the fcc/bcc metal system.

References

[1] B.I. Birajdar, S.V. Shende, and D.S. Joag, Surf. Sci. 505, 285 (2002).
[2] M. Trzcinski, A. Bukaluk, M. Bürgener, and A. Goldmann, Surface Science 589, 192 (2005).
[3] Th. Duden, R. Zdyb, M.S. Altman, and E. Bauer, Surf. Sci. 480, 145 (2001).
[4] J. Kotaczkiewicz, E. Bauer, Surf. Sci. 366, 71 (1996).
[5] J. Kotaczkiewicz, E. Bauer, Surf. Sci. 256, 87 (1991).
[6] M.A.J. Allen and D. Venus, Surf. Sci. 477, 209 (2001).
[7] K. Reshoft, C. Jensen, and U. Kohler, Surf. Sci. 421, 320 (1999).
[8] P. D. Augustus and J.P. Jones, Surf. Sci. 64, 713 (1977).
[9] H. Gollisch, Surf Sci. 175, 249 (1986).
[10] T. Engel, P. Bornemann, and E. Bauer, Surf. Sci. 81, 252 (1979).
[11] A. Hitzkea, J. Günster, J. Koaczkiewiczb, V. Kemptera, Surf. Sci. 318, 139 (1994).
[12] E. Koetter, D. Drakova, and G. Doyen, Surf. Sci. 331-333, 679 (1995).
[13] D. S. Choi and D. H. Kim, Thin Solid Films, 520, 6012 (2012).
[14] D. S. Choi and D. H. Kim, Modern Phys, Lett. B, 23, 835 (2009).
[25] L. R. Clavenna and L. D. Schmidt, Surf. Sci. 22, 365 (1970).
[16] A. Zangwill, *Physics at Surface*, (Cambridge, New York, 1988), p. 428.
[17] D. S. Choi, R. Gomer, Surf. Sci. 230, 277 (1990).
[18] N. Moslemzadeh, S. D. Barrett, and J. Ledieu, Phys. Rev. B. 66, 033403 (2002).
[19] Kh. Zakeri, T.R.F. Peixoto, Y. Zhang, J. Prokop, and J. Kirschner, Surf. Sci. Lett. 604, L1 (2010).
[20] M. Bode, R. Pascal, and R. Wisendanger, Surf. Sci. 334, 185 (1995).
[21] G. L. Cassiday and G.R. Fowles, Analytical Mechanics, 6th ed. (Thomson, 1999), chapter 6.
[22] P.W. Tamm and L.D. Schmidt, J. Chem Phys. 51, 5352 (1969).